JOURNAL OF MATERIALS SCIENCE 21 (1986) 2812–2818

Spectroscopic, electrical and EPR studies of binary semiconducting oxide glasses containing 50 mol % V_2O_5

E. E. KHAWAJA, M. SAKHAWAT HUSSAIN*, M. A. KHAN, J. S. HWANG*
*Physics Department, and *Chemistry Department, University of Petroleum and Minerals, Dhahran, Saudi Arabia*

Recent measurements on the V_2O_5–GeO_2 glass system consisting of an equimolar mixture of V_2O_5 and GeO_2 revealed that increase in electrical conductivity of these glasses upon annealing could be attributed to the increase in V^{4+} and V^{3+} content which accompanied the microstructure formation. In the present work we report a similar study on V_2O_5–TeO_2 and V_2O_5–P_2O_5 glass systems. It was found that in tellurite glass V^{3+} content increased upon annealing and V^{4+} content remained unchanged. In phosphate glass some increase in V^{4+} and no significant change in V^{3+} contents were observed. V^{3+} and V^{4+} contents in glasses could be best estimated from optical and electron paramagnetic resonance spectra, respectively.

1. Introduction

For vanadium germanate glasses the electrical conductivity measured by Chung and Mackenzie [1] was much smaller than that measured by Rao [2], as was pointed out by Chung and Mackenzie. Khan *et al.* [3] measured electrical conductivity of annealed and unannealed vanadium germanate glasses. These measurements clearly elaborated the discrepancies in two results. The conductivity of annealed samples at room temperature was found to be about five orders of magnitude greater than that of the unannealed samples containing a similar amount of vanadium oxide. The increase in conductivity on annealing was attributed to the change in microstructure of the glasses. Recently, Khawaja *et al.* [4] reported a detailed study of 50 mol % vanadium germanate glasses using electron paramagnetic resonance (EPR), optical absorption, differential scanning calorimetry and electron diffraction techniques. They concluded that the increase in the electrical conductivity of the annealed samples could be attributed to the increase of reduced valence states of vanadium ions (V^{3+} and V^{4+}) which accompany the microstructure formation and are not due to the structural changes alone.

It has been suggested [5] that the glass-forming oxide might not be simply a non-interacting solvent in the conduction process as was described by Ioffe *et al.* [6] for the V_2O_5–P_2O_5 system. However, Dhawan *et al.* [7] have reported that the conductivity of tellurite glasses is slightly higher than the corresponding composition of phosphate glasses.

The objective of the present investigation was to look into the effect of glass-forming oxides on the electrical and optical properties of vanadate glasses containing 50 mol % GeO_2, TeO_2 and P_2O_5 and to study the effect of annealing on these properties of the glasses.

2. Experimental details

Glasses were prepared by heating dry mixtures of analytical grade chemicals in alumina crucibles. Prior to melting the mixture, the alumina crucible was placed in a furnace maintained at 300° C for 1 h in order to minimize material volatilization. The crucible was then transferred to a melting furnace maintained at a selected temperature, given in Table I. The melt was frequently stirred with an alumina rod. The homogenized melts were then cast on to a stainless steel plate. The samples were disc-shaped with diameter 2 cm and thickness about 2 mm.

Thin glass films, which were necessary for the optical and infrared measurements, were obtained by a blowing technique. The as-blown glass film was mounted on to a machinable glass ceramic specimen holder, this holder having the capability of being placed directly into an annealing furnace as well as a spectrophotometer.

Measurements of d.c. conductivity were made using evaporated gold electrodes, which make good ohmic contacts, and a guardring configuration to eliminate surface leakage current. A stabilized power supply was used to provide a voltage source, and circulating currents were measured using a Keithley 610C electrometer. The temperature of the sample was monitored using a chromel–alumel thermocouple attached to the sample.

The optical density of the samples was measured as a function of wavelength using a Varian DMS 90 spectrophotometer in the spectral range 350 to 900 nm. First, the measurement was made from unannealed (UN) sample in the form of thin blown film which was mounted on a glass ceramic holder and then from the same sample when it was annealed for 24 h at a temperature given in Table I.

Four glass samples were prepared for the EPR

0022–2461/86 $03.00 + .12

TABLE I Preparation, treatment and the C ratio of glasses

Composition	Temperature of melting, T (°C)	Time for which melt was maintained at T (h)	Sample* treatment	$C = \frac{V^{4+}}{V_{total}}$	Activation energy, E_a (eV)	d.c. conductivity at room temperature ($\Omega^{-1} cm^{-1}$)
†50 V_2O_5–50 GeO_2	1100	3	Unannealed (UN)	0.008	0.60	4×10^{-12}
†50 V_2O_5–50 GeO_2	–	–	Annealed (AN) at 300° C	0.015	0.29	6×10^{-6}
50 V_2O_5–50 TeO_2	900	4	UN	0.013	0.45	7×10^{-7}
50 V_2O_5–50 TeO_2	–	–	AN at 270° C	0.013	0.32	4×10^{-6}
50 V_2O_5–50 P_2O_5	900	3	UN	0.186	0.49	3×10^{-7}
50 V_2O_5–50 P_2O_5	–	–	AN at 300° C	0.214	0.43	6×10^{-7}

*Annealing time was 24 h.
†The data are from [4].

study. The first two samples consisted of an equimolar mixture of tellurium dioxide and vanadium pentoxide, unannealed and annealed, respectively. The remaining two samples consisted of an equimolar mixture of phosphorous pentoxide and vanadium pentoxide, unannealed and annealed, respectively. Powdered glass samples for EPR measurements were prepared in capillary tubes. A typical sample contained approximately 50 mg and had a length of 15 mm. The whole sample was inside the active region of the EPR cavity.

The EPR spectra at room temperature (21.5° C) were recorded on a Bruker ER 200D SRC spectrometer interfaced with an Aspect 2000 data system. The magnetic field sweep was controlled with an ER 030 Hall effect field controller to 0.1 G and the magnetic field was measured with an ER 035M NMR Gaussmeter with an accuracy of 2 mG. The frequency was measured with a Model 5342A Hewlett–Packard frequency counter. The modulation amplitude and the modulation frequency employed were 3.2 G and 100 kHz, respectively. Both microwave power and modulation amplitude were verified to be at least ten times below the onset of broadening. The scan speed and time constant were chosen so as not to introduce any artefact by scanning. Spectra were all signal-averaged three times to increase the signal-to-noise ratio. Recorded spectra were digitized to 2000 points and stored on data cartridges for future analysis. Double integration of the first derivative spectrum was performed to obtain the spectral intensity. V^{4+} concentration was determined by comparing its spectral intensity with that of a bar-like synthetic ruby (SRM 2601) purchased from National Bureau of Standards. Both the sample and the ruby SRM were mounted on a 4 mm diameter quartz rod; the sample was tied to the quartz rod with a rubber band, while the ruby SRM was glued at the bottom of the rod with H_0 perpendicular to the c-axis. The resonance at 5360 G was used as the standard resonance.

Infrared absorption spectra in the range 4000 to 200 cm^{-1} were recorded on a Perkin–Elmer spectrophotometer Model 180. The spectra of the equimolar mixtures of the pure oxides were taken by mixing with an excess of dry KBr and then forming clear pellets of uniform thickness. The pellets for V_2O_5/P_2O_5 equimolar mixture could not be prepared because of very rapid absorption of moisture. The infrared spectra of the glass samples were obtained by holding the thin glass films in a specially designed sample holder in the sample compartment of the spectrometer. The same film was annealed in the sample holder and the spectra of the annealed sample were recorded.

3. Results

3.1. Conductivity

Fig. 1 shows the temperature variation of electrical conductivity of unannealed (UN) and annealed (AN) samples of V_2O_5–GeO_2, V_2O_5–TeO_2 and V_2O_5–P_2O_5 glasses. The data for V_2O_5–GeO_2 are from Khan *et al.* [3]. The measured conductivity for (UN) and (AN) samples of V_2O_5–P_2O_5 glass show little difference. It is clear from Fig. 1 that increase in conductivity on annealing is much larger in germanate glass compared to that in tellurite glass. In general, the data are in good agreement with those reported in the literature [1–3, 7]. The values of the activation energy as shown in Table I were calculated from the slopes of the curves, using the relation $\sigma = \sigma_0 \exp(-E_a/kT)$.

3.2. Optical absorption

Fig. 2 shows plots of optical density against wavelength of (UN) and (AN) samples of V_2O_5–GeO_2 [4], V_2O_5–TeO_2 and V_2O_5–P_2O_5 glasses. In V_2O_5–P_2O_5 glass the spectra for (UN) and (AN) samples were almost identical. It may be mentioned that the measurements in a given glass system are for the same sample, made before and after annealing. Again, it is apparent from Fig. 2 that the increase in optical absorption on annealing is much larger in germanate glass as compared to that in tellurite glass. The general appearance of the absorption spectra (Fig. 2) for all glasses is similar to each other and to those observed from other vanadium glasses [8, 9].

3.3. Electron paramagnetic resonance

The EPR spectrum of (UN) sample of TeO_2–V_2O_5 glass in Fig. 3 shows the typical hyperfine structure of an unpaired 3d electron in an axially distorted crystal field [10–12]. After annealing, the same features as in Fig. 3 remained. The spin concentrations of (UN) and (AN) samples were 4.62×10^{19} spins/g sample and 4.58×10^{19} spins/g sample, respectively. In fact, both samples have almost identical spin concentrations. The ratio $C = V^{4+}/V_{total}$ was found to be 0.013.

The EPR spectrum of (UN) sample of V_2O_5–GeO_2 [4] showed a similar hyperfine structure. However, the spectrum for the (AN) sample showed a featureless broad peak [4].

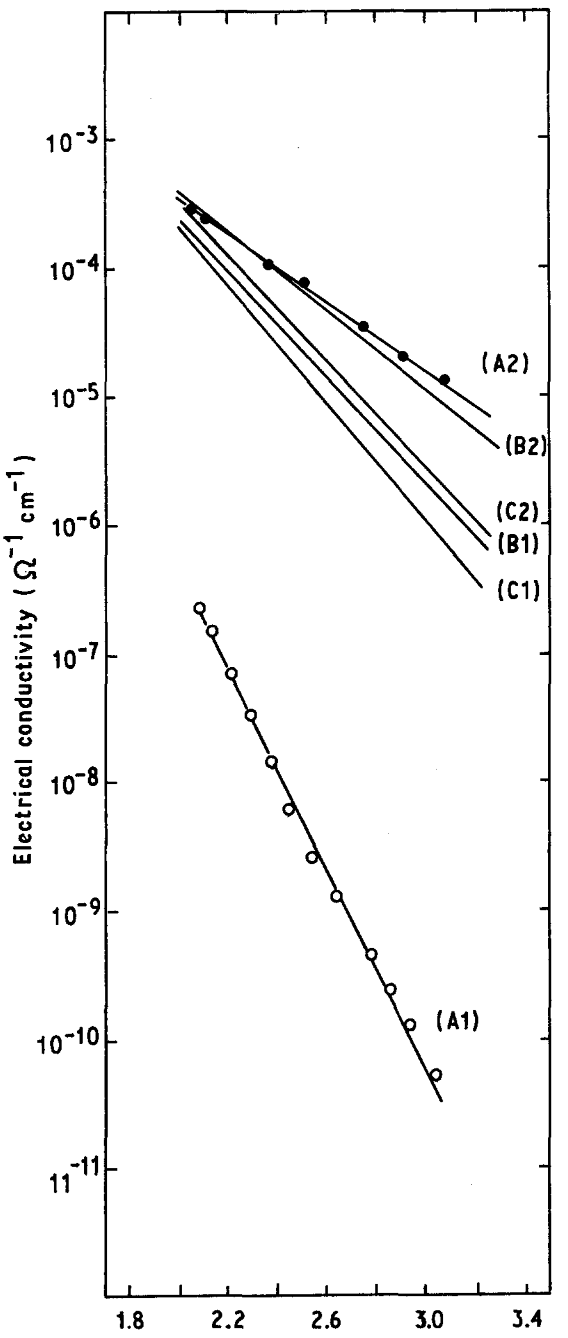

Figure 1 Electrical conductivity as function of reciprocal temperature for (A1) unannealed V_2O_5–GeO_2, (A2) annealed V_2O_5–GeO_2, (B1) unannealed V_2O_5–TeO_2, (B2) annealed V_2O_5–TeO_2, (C1) unannealed V_2O_5–P_2O_5 and (C2) annealed V_2O_5–P_2O_5 glass system.

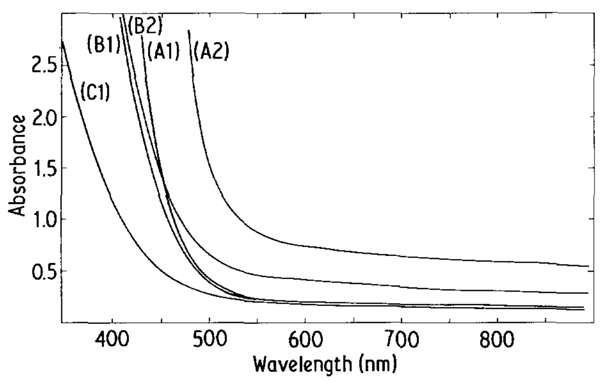

Figure 2 Optical absorption spectra for (A1) unannealed V_2O_5–GeO_2, (A2) annealed V_2O_5–GeO_2, (B1) unannealed V_2O_5–TeO_2, (B2) annealed V_2O_5–TeO_2, and (C1) annealed and unannealed V_2O_5–P_2O_5 glass films. Thicknesses of the films were about (A) 2.6 μm, (B) 2.0 μm and (C) 1.2 μm.

Fig. 4 depicts the EPR spectrum of an (UN) sample of V_2O_5–P_2O_5 glass. The spectrum of (AN) glass was similar to that of (UN) glass. Both showed a featureless broad line of width 299 and 307 G, respectively. The C values of (UN) and (AN) samples are listed in Table I along with those for other glasses.

Temperature-dependent linewidth studies were carried out for the (UN) glass sample of V_2O_5–TeO_2. At 208° C, the spectral lineshape is identical to that at room temperature. The spectrum remained well resolved up to a temperature of 270° C. Similar temperature-dependent studies were carried out with the (UN) as well as the (AN) sample of V_2O_5–P_2O_5 samples. The EPR spectra of both the unannealed and the annealed samples exhibit a strong temperature dependence. The EPR spectrum always exhibited a non-resolved single line whose linewidth increased with increasing temperature, with the (AN) sample showing slightly larger linewidths in comparison to that of the (UN) sample at the same temperature. While the linewidth of the unannealed sample decreased to a minimum of 243 G at −80° C, the linewidth of the annealed sample reached a minimum at 22° C and increased rapidly as the temperature decreased down to −176° C.

3.4. Infrared absorption

The spectral curves of the KBr discs for 1200 to 200 cm^{-1} range of the pure V_2O_5, TeO_2, GeO_2 and P_2O_5 are shown in Fig. 5 for ready reference. The spectra for the same region of KBr discs of equimolar mixtures, unannealed and annealed glass films of V_2O_5–TeO_2 and V_2O_5–GeO_2 glass samples are shown in Figs 6 and 7, respectively. The spectra of the V_2O_5–P_2O_5 glass sample are depicted in Fig. 8.

The infrared spectral data of the KBr pellets of all pure oxides agree with that reported in the literature [9, 13–17]. The V_2O_5–TeO_2 equimolar mixture spectrum (Fig. 6a) exhibits all characteristic absorptions for V_2O_5 and TeO_2. An absorption band at 1000 ± 10 cm^{-1} assigned to V=O stretching mode [9], was observed as a shoulder in the glass samples (Figs 6b

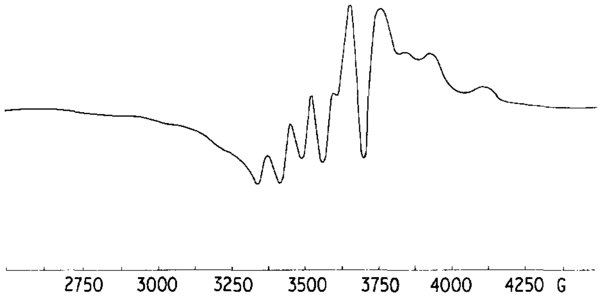

Figure 3 EPR spectrum of unannealed sample of V_2O_5-TeO_2. Sample weight = 46.72 mg. Spectrometer settings were as follows: signal average = three times; digitization = 2000 points; field set = 3500 G; scan range = 2000 G; scan time = 200 sec; mod. frequency = 100 kHz; mod. amplitude = 3.2 G; receiver gain = 2.5 × 10^4; time constant = 0.001 sec; microwave power = 6.4 mW; microwave frequency = 9.41 GHz.

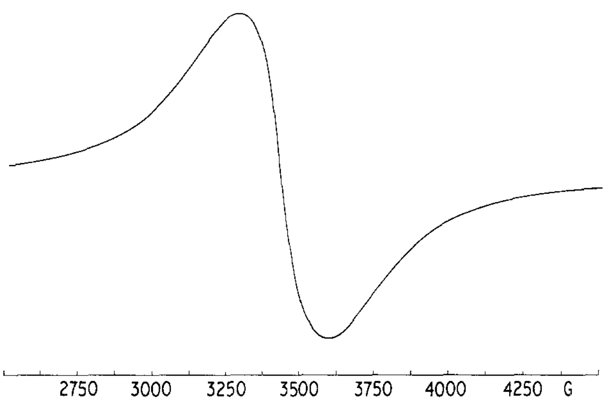

Figure 4 EPR spectrum of unannealed sample of V_2O_5–P_2O_5. Sample weight = 37.45 mg. Spectrometer settings were as follows: signal average = three times; digitization = 2000 points; field set = 3500 G; scan range = 2000 G; scan time = 200 sec; mod. frequency = 100 kHz; mod. amplitude = 3.2 G; receiver gain = 6.3×10^3; time constant = 0.001 sec; microwave power = 6.4 mW; microwave frequency = 9.41 GHz.

and c). The broad absorption at 825 cm^{-1} in crystalline V_2O_5 and at 780 cm^{-1} in crystalline TeO_2, appeared as a broad shoulder extending from 900 to 825 cm^{-1} in the glasses. Below 800 cm^{-1}, there are several strong absorption bands in crystalline V_2O_5 as well as in TeO_2. The two strong broad bands around 600 cm^{-1} in V_2O_5 assigned to V=O in-plane stretching and that at 650 cm^{-1} in TeO_2, are retained as a strong broad absorption centred at 675 cm^{-1} in the glass samples. The sharp peaks from 400 to 300 cm^{-1} in V_2O_5 and the broad band at 350 cm^{-1} in TeO_2 appeared as a weak and broad absorption centred at 325 cm^{-1}. The above data show that almost all absorptions observed in the crystalline oxide are retained as broad peaks or shoulders of relatively lower intensities in the amorphous V_2O_5–TeO_2 glass samples. The positions of the absorptions remained almost unaffected on glass formation. The disappearance of any new peaks indicates that the structural units in V_2O_5–TeO_2 glasses are the same as that in the pure V_2O_5 and TeO_2 oxides. Annealing of the V_2O_5–TeO_2 glass samples at 270° C revealed no change which was also in agreement with the EPR results on this system.

The infrared spectrum (Fig. 7a) of the KBr disc of equimolar mixture of crystalline V_2O_5 and GeO_2 is equivalent to a composite spectrum of the two oxides. The sharpness of the peaks in the crystalline material is retained in the spectrum of the equimolar mixture, as expected. In the glass samples of V_2O_5–GeO_2, the V=O stretching band at 1010 cm^{-1} was retained but the strong absorptions at 825 cm^{-1} in V_2O_5 and at 875 cm^{-1} in GeO_2 appeared as a broad absorption centred at 800 cm^{-1} (Fig. 7b). Instead of strong and sharp peaks at 600 cm^{-1} in V_2O_5 and at 550 cm^{-1} in GeO_2, a broad peak centred at 600 cm^{-1} with a shoulder at 475 cm^{-1} appeared in the equimolar mixture. This set of peaks in the region 600 to 500 cm^{-1} disappeared in the V_2O_5–GeO_2 glass system (Fig. 7b). The peaks below 500 cm^{-1} appeared as weak and broad absorptions in the glass samples. The infrared data of the V_2O_5–GeO_2 glasses is thus different from the composite spectra of the two oxides indicating the formation of different structural units in the glass samples than that in the starting materials. This behaviour is different from the V_2O_5–TeO_2 glass samples. Annealing of the V_2O_5–GeO_2 glass sample at 300° C clearly indicated microstructure formation. The spectrum of the annealed samples (Fig. 7c) was almost superimposable on that of the equimolar mixture (Fig. 7a) of the individual constituents. The microstructure formation in V_2O_5–GeO_2 glasses was also supported by the EPR measurements on these glass samples [4].

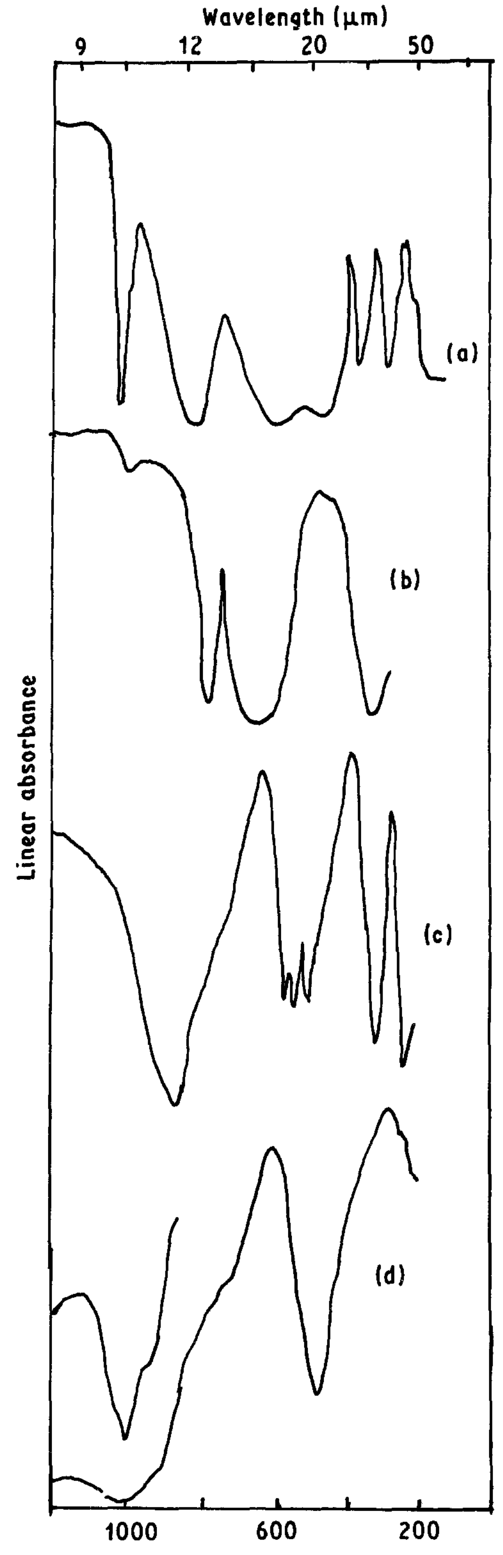

Figure 5 Infrared absorption spectra: (a) pure V_2O_5 crystalline, (b) TeO_2 powder, (c) GeO_2 powder, (d) P_2O_5.

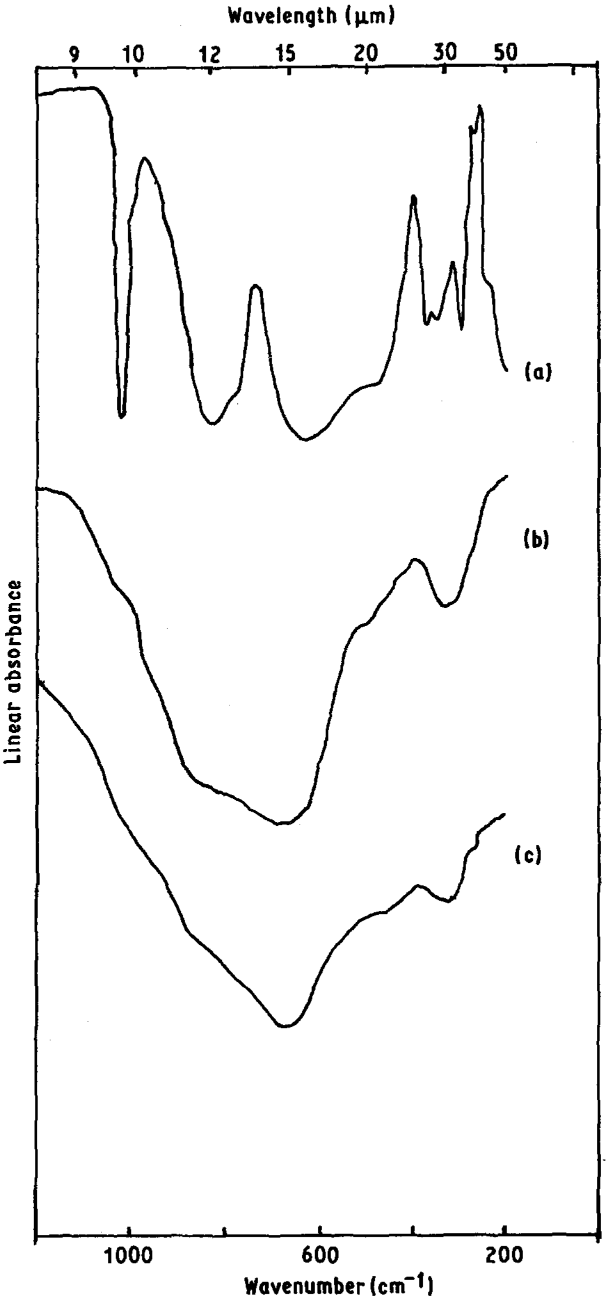

Figure 6 Infrared absorption spectra: (a) equimolar mixture of TeO_2 and V_2O_5 powders, (b) V_2O_5–TeO_2 glass before annealing, and (c) V_2O_5–TeO_2 glass film after annealing.

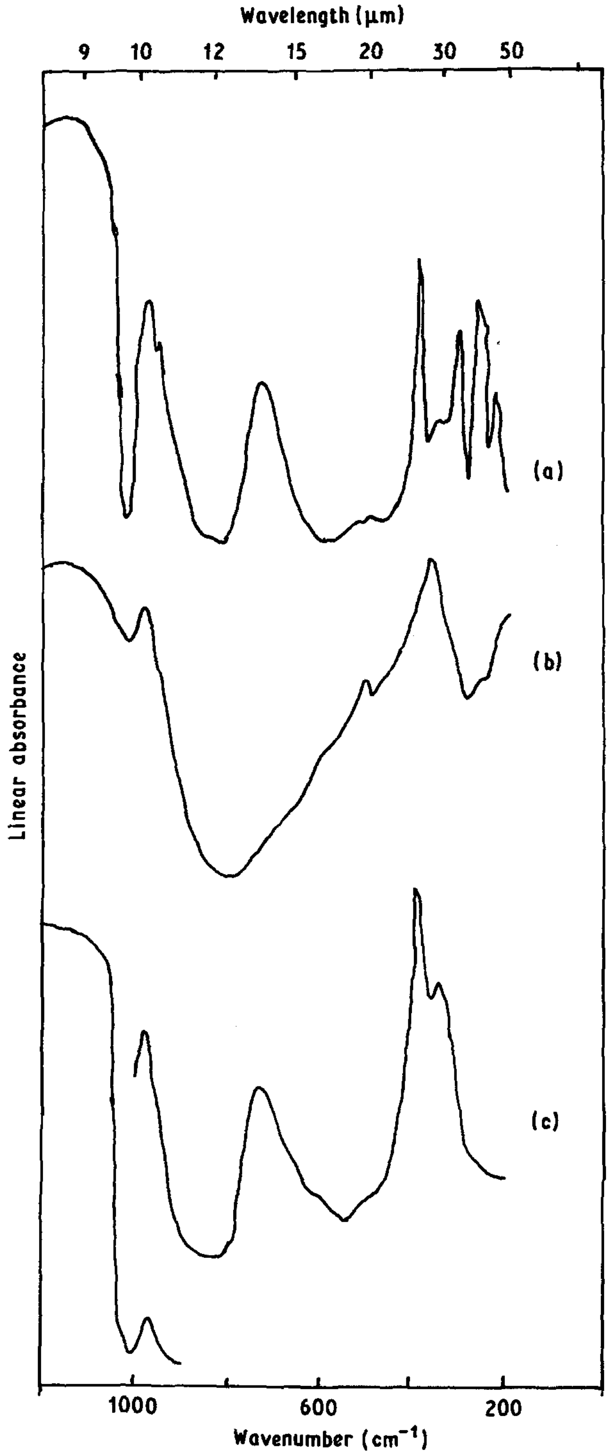

Figure 7 Infrared absorption spectra: (a) equimolar mixture of V_2O_5–GeO_2 powders, (b) unannealed V_2O_5–GeO_2 glass film, (c) V_2O_5–GeO_2 glass film after annealing.

The sharp peak at 1020 cm^{-1} with a shoulder at 940 cm^{-1} assigned to the P=O stretching mode in P_2O_5 and the V=O stretching absorption at 1010 cm^{-1} in V_2O_5, appeared as a strong band centred at 1025 cm^{-1} with one shoulder at 950 and another at 1150 cm^{-1} in the corresponding V_2O_5–P_2O_5 glass sample. The intensities of the 800 and 600 cm^{-1} peaks in pure V_2O_5 were reduced to two shoulders at 780 and 600 cm^{-1} (Fig. 8a) in the glass samples whereas the absorption at 460 cm^{-1} in P_2O_5 (Fig. 5d) remains unchanged in the glass sample. Similar to the V_2O_5–TeO_2 system, no new absorptions were observed nor were the positions of the absorptions in the constituents significantly changed in the V_2O_5–P_2O_5 glass sample. Annealing of the sample revealed no appreciable microstructure formation, although a slight splitting of the 460 cm^{-1} band occurred and a shoulder at 500 cm^{-1} appeared (Fig. 8b) in the annealed glass sample. This is probably indicative of an increase in the V_2O_4 concentration similar to the effects observed in the V_2O_5–GeO_2 glass system. However, the effects are much less pronounced in V_2O_5–P_2O_5 glass compared to the glass formed by addition of GeO_2 as glass former. The EPR data also show a slight increase in the spin concentration of V_2O_4 in the V_2O_5–P_2O_5 glass which supports our observation.

4. Discussion

It is clear from Figs 1 and 2 that in germanate and tellurite glasses electrical conductivity and optical absorption increased upon annealing the samples, while in phosphate glass the conductivity increased

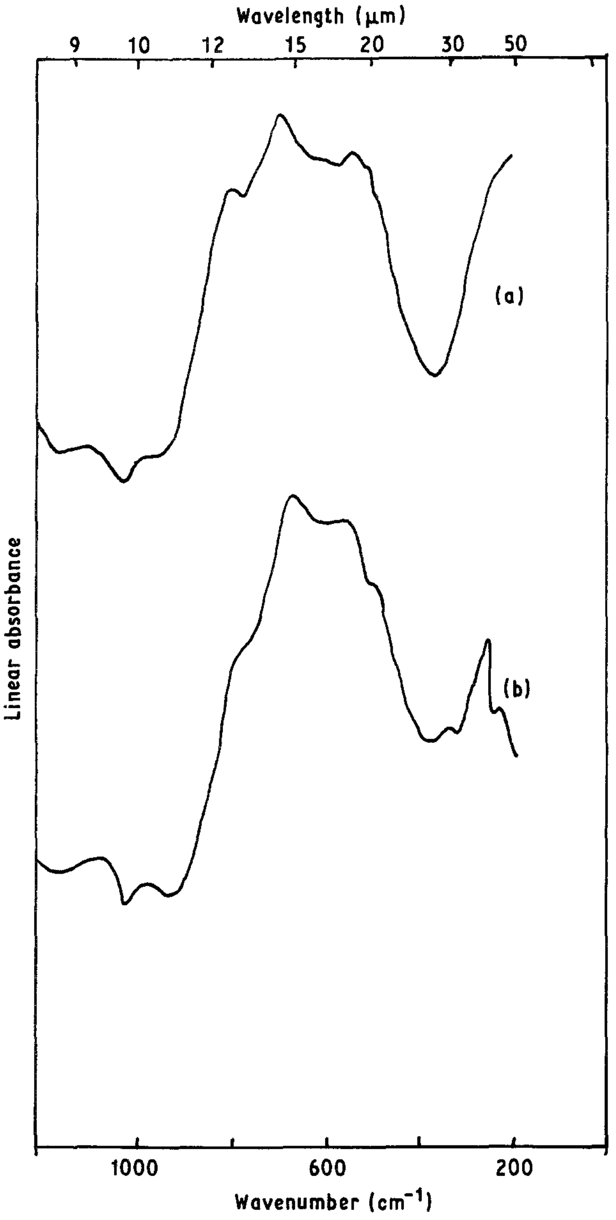

Figure 8 Infrared absorption spectra: (a) unannealed V_2O_5–P_2O_5 glass film, (b) V_2O_5–P_2O_5 glass film after annealing.

but the absorption remained unchanged. Upon annealing, V^{4+} content increased in germanate and phosphate glasses and remained unchanged in tellurite glass (Table I). The evidence of structural change on annealing has been confirmed in germanate glass by electron diffraction and EPR studies [4] and in the present infrared investigations. The present EPR and infrared studies suggest that annealing produces no appreciable change in the structure of tellurite and phosphate glasses.

However, Chung and Mackenzie [1] reported that the electrical conductivity of 55 V_2O_5–45 TeO_2 glass depends upon a second heat treatment at 270° C. The activation energies for the conduction of their glasses decreased from 0.37 eV to a constant minimum value of 0.19 eV with increasing time. We observed a similar decrease (Table I). According to them, the heat treatment did not alter the *C* value significantly (again this is in agreement with the present investigation – Table I) and the variation is a consequence of the difference in microstructure. Muncaster and Parke [18] also reported that in V_2O_5–TeO_2 glasses, annealing treatment had little effect on EPR spectra. They observed hyperfine structure similar to that shown in Fig. 3.

Limb and Davis [19] observed changes in microstructure in V_2O_5–P_2O_5 glasses as a result of heat treatment. They found that the concentration of V^{4+} was essentially independent of the temperatures of annealing and crystallization. However, we found a slight change in the V^{4+} content, upon annealing (Table I).

Therefore, it may be possible that in our investigations there was, upon annealing, some microstructure formation in tellurite and phosphate glasses, but EPR and infrared techniques were not sensitive enough to detect these. The other possibility is that the changes were too small to be detected by these techniques. It may be mentioned that we observed softening of tellurite glass at about 290° C.

The increase in the conductivity (Fig. 1) upon annealing as suggested by Chung and Mackenzie is a consequence of the difference in microstructure. However, we suggested earlier [4] that in the V_2O_5–GeO_2 glass system, the increase in conductivity may be due to the increase of reduced valence states of vanadium ions (V^{4+} and V^{3+}) which accompany the microstructure formation and are not due to the structural change alone. As discussed below, the present investigations support our view.

The general appearance of the absorption spectrum for the three glasses, keeping in mind the specimen thickness, is similar (Fig. 2). The glass former, therefore, has very little effect on the absorption. It is clear from the figure that absorption is increased upon annealing in germanate and tellurite glasses while it remained unchanged in phosphate glass. As suggested earlier [4] the possible effects responsible for this change may be (a) microstructure formation, (b) valency change in vanadium ions, or (c) the combination of both, which take place on annealing.

A reduced long wavelength tail (wavelength range from 500 to 900 nm, Fig. 2) is expected from the formation of the microstructure alone [4]. However, Fig. 2 shows results contrary to this, suggesting that microstructure formation alone is not responsible for the change in the optical spectrum.

It was reported by Bamford [20] that vanadium in the soda–lime–silica glass system, can exist in three oxidation states, namely V^{5+}, V^{4+} and V^{3+}. The absorption band at 350 nm was assigned by them to V^{5+}, the bands at 425 and 645 nm to V^{3+} and the band at 1100 nm to V^{4+}. The spectrum given by Bamford (Fig. 2.8 in [20]) indicates that absorption in the region from 400 to 900 nm has a major contribution from V^{3+} ions with possibly a small contribution from the tail of the band at 1100 nm, associated with V^{4+}. The bands shown in this figure are well resolved because the V_2O_5 content in these glasses is very small (0.5 wt %). In our glasses, since the V_2O_5 content is about a hundred times more, it is therefore expected that the bands would not be resolved. It follows from the above that the increase in the absorption tail (Fig. 2) in germanate and tellurite glasses, upon annealing is indicative of increased V^{3+} content in the glasses, whereas the V^{3+} content in phosphate glass does not change.

Therefore, the increase in electrical conductivity upon annealing may be attributed in germanate glass, to the increase in V^{3+} and V^{4+} content, in tellurite glass to the increase of V^{3+} content alone, and in phosphate glass to the increase of V^{4+} content alone. The valency changes may therefore be associated with microstructure formation of the samples upon annealing. Plausible explanations for the increase in concentration of V^{3+} and V^{4+} ions upon annealing were given by Khawaja *et al.* [4].

5. Conclusion

In vanadate glasses, glass former has little effect on electrical conductivity of these glasses, after appropriate heat treatment. This is in agreement with the findings of Ioffe *et al.* [6] and Dhawan *et al.* [7]. The conduction in these glasses possibly occurs by the movement of carriers from the lower valency state to the higher valency state (i.e. $V^{3+} \rightarrow V^{4+}$ and $V^{4+} \rightarrow V^{5+}$).

The increase in electrical conductivity of these glasses upon annealing could be attributed to the increase of reduced valence states of vanadium ions which may accompany the microstructure formation and is not due to the structural change alone.

It was found that V^{3+} and V^{4+} content in the glasses could be best estimated by optical absorption and EPR techniques, respectively.

Acknowledgement

We wish to acknowledge the support of UPM Research Committee.

References

1. C. H. CHUNG and J. D. MACKENZIE, *J. Non-Cryst. Solids* **42** (1980) 357.
2. B. V. J. RAO, *J. Amer. Ceram. Soc.* **48** (1965) 311.
3. M. N. KHAN, E. E. KHAWAJA, D. SAVE, A. A. KUTUB and C. A. HOGARTH, *Int. J. Electron.* **56** (1984) 395.
4. E. E. KHAWAJA, J. S. HWANG, F. TEGALLY, A. A. KUTUB and A. S. W. LI, *J. Mater. Sci.* **20** (1985) 3074.
5. B. W. FLYNN, A. E. OWEN and J. M. ROBERTSON, Proceedings of the International Conference on Amorphous and Liquid Semiconductors, edited by W. E. Spear (CICL, Edinburgh, 1977) p. 678.
6. V. A. IOFFE, J. B. PATRINA and I. S. POBEROVSHAYA, *Sov. Phys. Solid State* **2** (1960) 609.
7. V. K. DHAWAN, A. MANSINGH and M. SAYER, *J. Non-Cryst. Solids* **51** (1982) 87.
8. C. A. HOGARTH and A. A. HOSSEINI, *J. Mater. Sci.* **18** (1983) 2697.
9. G. W. ANDERSON and W. D. COMPTON, *J. Chem. Phys.* **52** (1970) 6166.
10. C. SANCHEZ, F. BABONNEAU, R. MORINEAC, J. LIVAGE and J. BULLOT, *Phil. Mag. B* **47** (1983) 279.
11. A. K. BANDYOPADHYAY, M. RIBES, F. OPERNOT and Z. ZARZYCKI, *Phys. Chem. Glasses* **23** (1982) 31.
12. H. HENRI, C. SANCHEZ, C. R'KAH and J. LIVAGE, *J. Phys. C. Solid State Phys.* **14** (1981) 829.
13. C. SANCHEZ, J. LIVAGE, J. P. ANDIERE and A. MADI, *J. Non-Cryst. Solids* **65** (1984) 285.
14. C. A. HOGARTH and G. R. MORIDI, *J. Mater. Sci. Lett.* **3** (1984) 481.
15. K. KNEIPP, H. BURGER, D. FASSLER and W. VOGAL, *J. Non-Cryst. Solids* **65** (1984) 223.
16. M. M. AHMED, C. A. HOGARTH and M. N. KHAN, *J. Mater. Sci.* **19** (1984) 4040.
17. M. SAYER and A. MANSINGH, *Phys. Rev. B* **6** (1972) 4629.
18. R. MUNCASTER and S. PARKE, *J. Non-Cryst. Solids* **24** (1977) 399.
19. Y. LIMB and R. F. DAVIS, *J. Amer. Ceram. Soc.* **62** (1979) 403.
20. C. R. BAMFORD, "Colour Generation and Control in Glass" (Elsevier, Amsterdam, 1977) p. 52.

Received 15 April
and accepted 3 October 1985